4th Micro and Nano Flows Conference
UCL, London, UK, 7-10 September 2014

Stretching of a capillary bridge featuring a particle-laden interface: particle sedimentation in the interface

Lorenzo Botto

School of Engineering and Materials Science, Queen Mary University of London, E1 4NS, UK

Abstract Colloidal particles adsorbed at fluid interfaces can be subject to external forces, for instance of magnetic, electrical, or gravitational origin. To develop a tool that will enable to study the effect of these forces on interfacial particle transport, we derive a transport equation for the surface particle concentration using the method of volume averaging. This equation is specialised to the problem of particle sedimentation induced by external forces on an axisymmetric capillary bridge stretched with assigned constant velocity between two circular plates. The equation for the interfacial concentration is one-way coupled to the unsteady Stokes equation in the capillary bridge, and solved in the thin-thread approximation, in the limit of small capillary and Bond numbers and for moderate area fractions. We find that owing to the competition between particle settling in one direction, and fluid velocity in the opposite direction, a concentration peak develops between the neck region and the moving plate. Hydrodynamic interactions, modelled through a concentration-dependent hindrance function, have the effect of steepening the shock-like concentration gradients that develop in the interface.

Keywords: Suspensions, Colloids, Interfacial Flows, Averaged Multiphase-Flow Equations

1. Introduction

Solid particles of intermediate wettability have a tendency to adhere to fluid interfaces. This phenomenon is purely mechanical in nature, and is due to capillary forces holding the particles at an equilibrium position in the interface ([1]). The strong attachment of particles to fluid interface is exploited in a variety of applications, from solid-stabilised emulsions and foams, to froth flotation, to the development of new materials, where the particles are primarily used to alter the effective mechanical properties of the interface or prevent coalescence ([2, 3, 4]).

One of the most distinctive characteristics of solid particles (as opposed to surfactants) is the facility with which they can be designed to respond to external forces. It has been suggested that the interfacial transport of particles by external fields (e.g. magnetic) can be a useful strategy to modify dynamically the mechanics of interfaces ([5]), but so far the amount of fundamental work done on the topic is very limited ([6, 7, 5]). In addition, there is a need to study the important effect of gravitational settling on the ageing properties of particle-laden interfaces [6, 7]. As a step towards understanding interfacial particle transport by external field, in this work we consider the problem of an axisymmetric liquid bridge stretched between two disks, translating parallel to each other with an assigned constant velocity. The liquid bridge comprises a viscous fluid immersed in a second fluid of negligible viscosity (e.g., air). The interface of the bridge is populated with rigid particles, which migrate owing to a constant external field directed parallel to the bridge axis . The problem of the stretched liquid bridge has been extensively studied in the case of clean (see, e.g., [8, 9]), and surfactant-covered interfaces ([10, 11]). It therefore constitute a useful starting point a broad investigating on the effect of external forces on interfacial particle transport.

A contribution of this work is the systematic development of a transport equation for the particle concentration in the interface. While we include only the term corresponding to a con-

stant external force, the formulations is general, and can accommodate inter particle interactions of hydrodynamic and non-hydrodynamic origin. The transport equation for the particle concentration is one-way coupled to the unsteady Stokes equation for the flow within the liquid bridge. Both the unsteady Stokes equation and the transport equation for the particle concentration are solved in the thin-thread approximation. We are specifically interested in the competition between particle settling in one direction, and stretching of the bridge in the opposite direction, and in the effect that these competing factors have on the particle concentration field.

2. Description of the problem

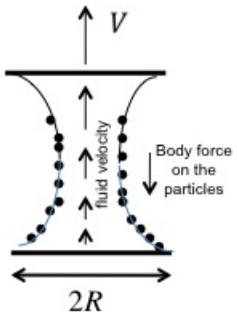

Figure 1: Sketch of the problem

We consider an axisymmetric liquid bridge held captive between two identical circular disks of radius R (see Fig.1). The interface of the bridge separates an inner fluid of viscosity μ from an outer fluid of viscosity $\mu_o \ll \mu$. It will be assumed that the dynamical influence of the outer fluid on the bridge is negligible. A cylindrical coordinate system (r,z) is set fixed to the lower disk, with the origin at the disk's centre and $z-$ axis directed upwards.

The interfaces is populated with identical spherical particles of radius a. The particles are adsorbed making a contact angle of 90° with the interface. Under this condition the particles are half-immersed in each fluid.

Starting with a cylindrical liquid bridge of length L_0, a constant upward velocity V is applied to the top boundary, while the bottom boundary is kept fixed. The particles are acted upon by an external force that makes the particles sediment downwards. The inertia of the fluid and the particles is neglected.

3. Results and discussion

3.1 Derivation of a transport model for the particle concentration

Colloidal particles - unlike surfactant molecules - are characterised by well-defined boundary conditions at their surfaces, and can be acted acted upon by external and inter-particle forces that, in many cases, can be calculated from first principles. Modelling their transport does not, therefore, require to postulate phenomenological equations: these equations can be derived systematically, using standard averaging techniques developed for multiphase flows. In this section we use the method of volume averaging to derive a transport equation similar to the suspension-balance model for bulk suspensions discussed by Nott & Brady ([12]).

To apply volume averaging, we consider the particle-fluid "mixture" contained within a thin control volume that embeds the interface. For convenience of analysis this control volume is taken to be a rectangular prism of thickness ε and side length l_v, with $\varepsilon \ll l_v$, having the wider face parallel to the interface. The control volume is assumed to comprise a sufficient number of particles that a continuum treatment is justified.

The continuity and momentum equations, valid both within the region occupied by the solid and the region occupied by the fluids, are $\frac{\partial \rho}{\partial t} + \nabla \cdot \rho \mathbf{u} = 0$ and $\nabla \cdot \boldsymbol{\sigma} + \mathbf{b} = 0$, respectively, where $\mathbf{u}$ is the velocity vector, $\boldsymbol{\sigma}$ is the stress tensor, and $\mathbf{b}$ is an external force. A convenient way to obtain the continuity equation for the particle phase is to multiply the continuity equation given above by an indicator function X, which is one inside the particles and zero otherwise, and then volume average over the volume V occupied by the control volume. We will use the notation $\langle \cdot \rangle = 1/V \int_V (\cdot) dV$ to denote volume averaging. It is easy to show (see

[13]) that this formal procedure leads to

$$\frac{\partial \phi}{\partial t} + \nabla \cdot \phi \left\langle \mathbf{u} \right\rangle_p = 0, \qquad (1)$$

where $\left\langle \mathbf{u} \right\rangle_p = \phi^{-1} \left\langle \mathbf{u} \right\rangle$ is the phase-averaged particle velocity and $\phi = \langle X \rangle$ is the particle volume fraction.

The particles are constrained to move along the fluid interface. Since spatial derivatives are taken along the interface, the nabla operator ∇ can be replaced by the corresponding surface operator ∇_s (the two operators applied to a tangential field give the same result). Moreover, because Eq. (1) is linear in the concentration, ϕ can be replaced by the surface fraction ϕ_s, giving $\frac{\partial \phi_s}{\partial t} + \nabla_s \cdot \phi_s \left\langle \mathbf{u} \right\rangle_p = 0$. This equation models the change in concentration of particles in a control volume whose lateral area (the area obtained by projecting the control volume region onto the undisturbed interface) is fixed. This formulation is suitable for a flat interface. When the interface is curved the lateral area of the control volume changes at a rate equal to KU_n, where K is the total (twice the mean) curvature of the interface and U_n is the normal velocity of the interface ([14]). For a curved interface, Eq. (**??**) should therefore be amended with a curvature term, leading to

$$\frac{\partial \phi_s}{\partial t} + KU_n\phi_s + \nabla_s \cdot \phi_s \left\langle \mathbf{u} \right\rangle_p = 0. \qquad (2)$$

Note that Eq.(2) contains the particle velocity, not the fluid velocity; this important difference is often overlooked in the literature on surfactants.

Volume averaging the momentum equation gives rise to the average stress inside the particles $\nabla \cdot \langle X\boldsymbol{\sigma} \rangle$, the interfacial momentum source term $\langle \nabla X \cdot \boldsymbol{\sigma} \rangle$, and the volume average body force acting on the particles, $\langle \mathbf{b} \rangle$ ([12]). The average stress within the particles can be decomposed ([15]) as $\langle X\boldsymbol{\sigma} \rangle = \boldsymbol{\Sigma} + \langle \mathbf{xb} \rangle$, where $\boldsymbol{\Sigma} = \frac{1}{V} \int_{S_p} \mathbf{x}\boldsymbol{\sigma} \cdot \mathbf{n} dS$ is the stresslet giving rise to the "effective viscosity" of the suspension, and $\langle \mathbf{xb} \rangle$ is the Irving-Kirkwood tensor that models non-hydrodynamic interparticle interactions ([12]). The interfacial momentum source term, as in a bulk suspension, is just the volume average value of the hydrodynamic and hydrostatic forces that the particles exert on the fluid within the control volume. We denote the forces per unit volume due to hydrostatic and hydrodynamic forces by $\mathbf{F}_{hs}$ and $\mathbf{F}_{hd}$, respectively. With this notation the momentum balance reads $\nabla_s \cdot \langle \boldsymbol{\Sigma} \rangle + \nabla_s \cdot \langle \mathbf{xb} \rangle + \mathbf{F}_{hs} + \mathbf{F}_{hd} + \langle \mathbf{b} \rangle = 0$. Upon multiplication by the control volume thickness the average momentum equation for the particle phase becomes

$$\nabla_s \cdot \boldsymbol{\Sigma}_s + \nabla_s \cdot \langle \mathbf{xb} \rangle_s + \boldsymbol{\tau}_{hs} + \boldsymbol{\tau}_{hd} + \langle \mathbf{b} \rangle_s = 0 \quad (3)$$

where $\langle \cdot \rangle_s = 1/A \int_V (\cdot) dV$, with $A = l_v^2$. The vectors $\boldsymbol{\tau}_{hs}$ and $\boldsymbol{\tau}_{hd}$ are the surface stresses corresponding to $\mathbf{F}_{hs}$ and $\mathbf{F}_{hd}$, respectively, and $\boldsymbol{\Sigma}_s = \frac{1}{A} \int_{S_p} \mathbf{x}\boldsymbol{\sigma} \cdot \mathbf{n} dS$. The physical meaning of Eq. (3) is quite clear if the term $\boldsymbol{\Sigma}_s$ is neglected. In this case, Eq. (3) expresses a balance between the hydrodynamic, hydrostatic, and body forces acting on the particles and the tension in the plane of the interface owing to inter-particle interactions of non hydrodynamic origin.

In order to couple the average continuity equation (2) with the momentum equation (3), the term $\boldsymbol{\tau}_{hd}$ originating from the shear forces on the interfacial particles due to the bulk fluid motion, must be closed. It is reasonable to parameterise $\boldsymbol{\tau}_{hd}$ on the bulk fluid velocity extrapolated at the location of the interface, $\mathbf{U}_s$, because this quantity determines the magnitude of the shear forces acting on the portion of each particle surface in contact with the fluid of higher viscosity. Because of Galilean invariance and linearity of the governing equations, $\boldsymbol{\tau}_{hd}$ must be proportional to $\left\langle \mathbf{u} \right\rangle_p - \mathbf{U}_s$. In addition, $\boldsymbol{\tau}_{hd}$ must depend on the dynamic viscosity of the fluid μ, the particle size a, and the average inter-particle separation ℓ. Dimensional analysis suggests $\boldsymbol{\tau}_{hd} = -F_1(\phi_s)\frac{\mu}{a}\left(\left\langle \mathbf{u} \right\rangle_p - \mathbf{U}_s\right)$ where F_1 is a non-dimensional function. When the particles are widely separated at a liquid-gas interface, the Stokes drag on each particle is equal to half that in the bulk ([16]). The drag force per unit area is thus approximately $3\pi\mu\frac{a}{\ell^2}\left(\left\langle \mathbf{u} \right\rangle_p - \mathbf{U}_s\right)$, which suggest that $F_1 \to 3\phi_s$ as $\phi_s \to 0$. This justifies writing

$$\boldsymbol{\tau}_{hd} \simeq -\frac{3\phi_s\mu}{f(\phi_s)a}\left(\left\langle \mathbf{u} \right\rangle_p - \mathbf{U}_s\right), \qquad (4)$$

where $f(\phi_s)$ is an hindrance function satisfying $f(0) = 1$ that accounts for hydrodynamic interactions. Using equations (4) and (3) the continuity equation (2) can be recast as

$$\frac{\partial \phi_s}{\partial t} + KU_n\phi_s + \nabla_s \cdot \phi_s \mathbf{U}_s = -\frac{a}{3\mu}\nabla_s \cdot f\left(\nabla_s \cdot \mathbf{\Sigma}_s + \nabla_s \cdot \langle \mathbf{xb} \rangle_s + \boldsymbol{\tau}_{hs} + \langle \mathbf{b} \rangle_s\right). \tag{5}$$

For a dilute suspension of force-free Brownian particles, $\mathbf{\Sigma}_s \propto -\phi_s \boldsymbol{I}$, where $\boldsymbol{I}$ is the identity tensor, and (5) reduces to a convection-diffusion equation. When a significant difference between the particle and fluid velocities occurs, and interparticle forces of non-hydrodynamic origin are absent, the drag and "buoyancy" terms dominate; thus

$$\frac{\partial \phi_s}{\partial t} + KU_n\phi_s + \nabla_s \cdot \phi_s \mathbf{U}_s = -\frac{a}{3\mu}\nabla_s \cdot f\left(\boldsymbol{\tau}_{hs} + \langle \mathbf{b} \rangle_s\right). \tag{6}$$

This equation can be rewritten as

$$\frac{\partial \phi_s}{\partial t} + KU_n\phi_s + \nabla_s \cdot \phi_s \left(\mathbf{U}_s + f\mathbf{U}_{p,0}\right) = 0 \tag{7}$$

where

$$\mathbf{U}_{p,0} = \frac{a\left(\boldsymbol{\tau}_{hs} + \langle \mathbf{b} \rangle_s\right)}{3\mu\phi_s}, \tag{8}$$

is the single-particle settling velocity In the case of gravitational sedimentation, $\phi_s^{-1}\langle \mathbf{b} \rangle_s$ is the particle weight and $\phi_s^{-1}\boldsymbol{\tau}_{hs}$ is the buoyancy force.

3.2 Thin-thread approximation

The thin-thread approximation consists in expanding all the flow variables in the slenderness parameter R/L_0 and retaining only the leading order terms ([17]). It is easy to show that the thin-thread approximation corresponding to Eq. (7) is

$$\frac{\partial \phi_s}{\partial t} + \frac{1}{2}\phi_s\frac{\partial u}{\partial z} + u\frac{\partial \phi_s}{\partial z} - U_{p,0}\frac{\partial}{\partial z}\left(f(\phi_s)\phi_s\right) = 0 \tag{9}$$

where $U_{p,0} = |\mathbf{U}_{p,0}|$ and u is the leading-order z-component of the fluid velocity. We assume $\mathbf{U}_{p,0}$ to be directed in the negative z direction. The simulations presented in the next section couple (9) with the thin-thread solution of the incompressible unsteady Navier-Stokes equation, as formulated in Eggers and Dupont ([17]). In contrast to these authors, we neglect the nonlinear convective term.

Marangoni stresses are not included in our numerical solution of the interfacial dynamics, the surface tension is assumed constant, and body forces acting on the interface are neglected. This is equivalent to a one-way-coupling approximation, in which the effect of the fluid on the particles is accounted for, but the effect of the particles on the fluid and the interface is neglected. The transport equation (9) is solved with the velocity field u provided by the solution of the unsteady Stokes equation. The resulting coupled system of nonlinear equations is solved on a fixed grid, using the transformation $\xi = z/L(t)$ to map the original problem defined on $z \in [0, L(t)]$ into an equivalent problem on $\xi \in [0,1]$. The coupled equations is discretised in time using a Crank-Nicholson scheme. The terms $u\frac{\partial \phi_s}{\partial z}$ and $U_{p,0}\frac{\partial}{\partial z}\left(f(\phi_s)\phi_s\right)$ are discretised by centered difference and by a first-order upwind scheme, respectively. Dirichlet boundary conditions for the velocity are used at $z = 0$ and $z = L$. Because the settling of the particle leaves clear fluid at $z = L$, we enforce $\phi_s(z = L, t) = 0$. Due to the hyperbolic character of the sedimentation equation, we do not impose boundary conditions for ϕ_s at $z = 0$, but calculate derivatives using interior points. For the simulations presented in this paper we used 64 discretisation points.

3.3 Numerical simulation of particle transport

The following parameters were used for the flow simulation: $L_0/R = 2.0, \rho VR/\mu = 0.03, \mu V/\gamma = 0.115$, and $\Delta\rho g R^2/\gamma = 0$, where ρ is the density of the inner fluid and $\Delta\rho$ is the density difference between the inner and outer fluids. These values approximate the conditions found in one set of experiments by Kroger et al. ([18]),

and the parameters used by Gaudet et al. ([9]) for one of their simulations. For these parameters, the flow and the interface are perfectly symmetric about the bridge midpoint location. Interface profiles are shown in Fig. 2 (a) and the corresponding axial velocities in Fig. 2 (b). Figure 3 shows the time evolution of the minimum radius, comparing with the work of Kroger et al. ([18]) and Gaudet et al ([9]). The agreement is reasonably good, in spite of the thin-thread approximation being applied to a short liquid bridge.

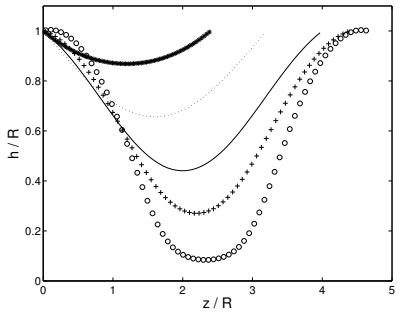

(a)

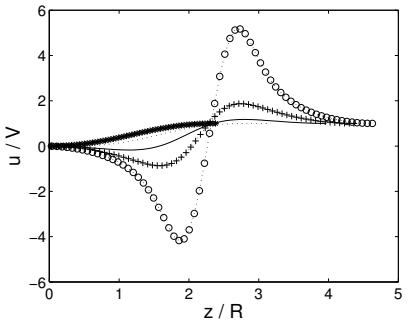

(b)

Figure 2: Radial interface profiles (a) and axial velocity profiles (b) vs axial coordinate for $tV/R = 0.0, 0.4, 1.2, 2.0, 2.4$ and 2.66

Figure 4 shows the concentration profile, solution of Eq. (9), corresponding to $U_{p,0} = 0$ and $\phi_{s,0} = 0.1$, for selected times corresponding to those in Fig. 2 (a). The parameter $\phi_{s,0}$ is the initial concentration, which for all the simulations in this paper is chosen to be uniform. Unless specified, the hindrance function f is set to 1.

It is seen that the curves in Fig. 4 and the corresponding ones in Fig. 2 (a) have the same shape. This is due to the fact that, for $U_{p,0} = 0$, Eq. (9) is identical to the equation governing

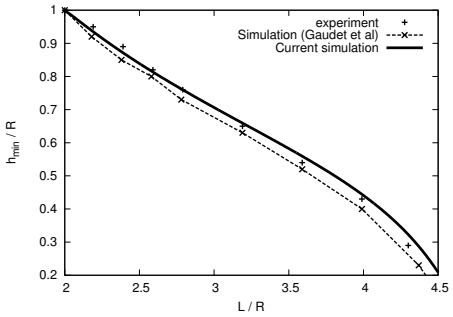

Figure 3: Minimum liquid bridge radius vs time, comparing with the experiment of Kroger et al. ([18]) and the simulation of Gaudet et al. ([9])

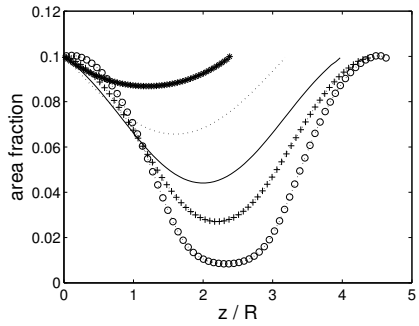

Figure 4: Time evolution of the concentration profile for $\phi_{s,0} = 0.1$ and $U_{p,0} = 0$. The curves correspond to those in Fig. 2 (b)

the interface profile $h(z,t)$, i.e.

$$\frac{\partial h}{\partial t} + \frac{1}{2} h \frac{\partial u}{\partial z} + u \frac{\partial h}{\partial z} = 0. \qquad (10)$$

While the two governing equations are identical, the boundary conditions are not. However, we notice that the solution ϕ_s appears to be practically pinned to its initial value at $z = 0$ and $z = L$. This feature can be understood by noticing that, near $z = 0$, $u \simeq 0$ and $\frac{\partial u}{\partial z} \approx 0$ (see Fig. 2 b) because of the no-slip condition and the comparatively small curvature of the interface near $z = 0$. Because of these two conditions, Eq.9 yields $\frac{\partial \phi_s}{\partial t} \simeq 0$. The solution is thus approximately stationary near $z = 0$. A similar argument holds for the boundary at $z = L$.

The fluid velocity relative to the velocity of the neck is symmetric with respect to the neck location. It is expected that force-free particles follow the flow as passive scalars. The fact that a symmetric concentration profile corresponds

to a symmetric velocity profile is therefore a confirmation of the quality of the numerical solution.

Figure 5 (a) shows the effect of choosing a finite value $U_{p,0}/V = 0.1$ on the time-dependent concentration profile. Owing to settling the particles leave a zero-concentration clear fluid region, whose width increases slowly with time, near the boundary at $z = L$. Adjacent to the clear-fluid region a concentration maximum occurs. The concentration value corresponding to this maximum initially decreases, as the liquid bridge stretches producing more interfacial area. However, at later times the maximum value increases, because the particles are resuspended by the relatively large positive fluid velocity induced by the necking of the bridge. For the parameters considered the concentration profile away from the clear-fluid region is almost symmetric.

Figure 5 (b) shows the concentration profile corresponding to $tV/R = 2.66$ and different values of $U_{p,0}$. A concentration peak develops in the region between the neck and the moving boundary. It is expected that this region of particle accumulation will be present in the interface even after pinch-off (in our simulation $tV/R = 2.66$ is close to the pinch-off time). For $U_{p,0}/V$ larger than about 0.8-0.9, the peak disappears, because in this case the settling velocity is large enough that the resuspension mechanism described above becomes negligible. The concentration profile to the left of the neck appears to be only mildly affected by the value of the settling velocity.

In interpreting the results, one should take into account that, because the model does not include terms that enforce the no-overlapping condition between the particles and hydrodynamic diffusion terms, a large-concentration sedimentation layer of zero thickness must develop at $z = 0$. This concentration peak is not included in the plots, although its value can be easily computed from mass conservation.

Hydrodynamic interactions manifesting themselves in a concentration dependent settling velocity should have a significant effect on particle transport. The hindrance function

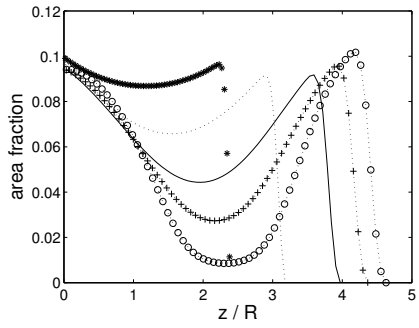

(a)

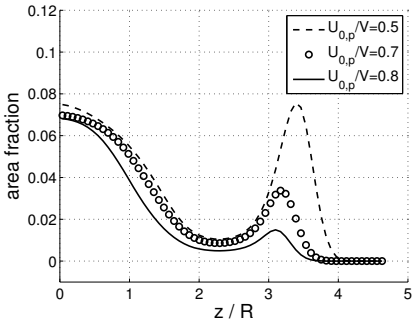

(b)

Figure 5: (a) Time evolution of the concentration profile for $\phi_{s,0} = 0.1$ and $U_{p,0} = 0.1$; (b) concentration profile for $tV/R = 2.66$ and different values of the single-particle settling speed

for particles immersed between a viscous fluid and a fluid of negligible viscosity can be estimated by noting that Eq. (4) corresponds to a Navier slip boundary condition with slip length $\lambda(\phi_s) = \frac{af(\phi_s)}{3\phi_s}$ in a frame of reference moving with velocity $\langle \mathbf{u} \rangle_p$. In their study of superhydrophobic surfaces, Davis and Lauga ([19]) calculated analytically the slip length for shear-flow over a square array of circular no-slip regions obtaining $f(\phi_s) = \frac{9\pi}{16} - \frac{9}{2\sqrt{\pi}} \ln((1+\sqrt{2}))\sqrt{\phi_s}$, an expression valid from small to moderate values of ϕ_s. The value $\frac{9\pi}{16}$ originates from the fact that the Stokes drag force on an isolated disk embedded in a shear-free interface is exactly $\frac{9\pi}{16}$ times as small as the Stokes drag for a half-immersed sphere having the same radius [20]. Therefore, a reasonable estimate for the hindrance function for spheres can be obtained by dividing Davis and Lauga's expression by a

factor $\frac{9\pi}{16}$:

$$f(\phi_s) \simeq 1 - \frac{8}{\pi^{3/2}} \ln((1+\sqrt{2}))\sqrt{\phi_s}. \quad (11)$$

The dependence on area fraction predicted by Eq. (11) is quite strong. For instance, the settling velocity of particles at $\phi_s = 0.1$ is approximately 40% smaller than the single-particle settling velocity.

Figure (6) shows the effect of modelling hydrodynamic interactions with Eq. 11 as opposed to simply assuming $f = 1$. Including hydrodynamic interactions has the effect of steepening the concentration gradients developing near the moving boundary. The steepening is more pronounced the larger the value of $\phi_{s,0}$. The particle settling velocity is a decreasing function of concentration. Particles near the clear fluid therefore move faster than those located at smaller values of z, leading to a steepening of the shock-like concentration profile.

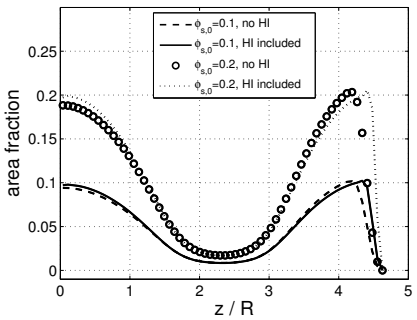

Figure 6: Effect of including hydrodynamic interactions (HI) on the concentration profile, $tV/R = 2.66$

4. Summary and conclusions

A transport equation for the surface concentration field for particles adsorbed on curved surfaces has been systematically derived, and applied to a numerical study of colloidal particles adsorbed on the interface of a stretched liquid bridge, held captive between a stationary circular disk and one moving at constant velocity V. The conditions are of small Reynolds, capillary, and Bond numbers. The particle dynamics is studied in the one-way coupling approximation in which the presence of the particles does not alter the evolution of the interface and the motion of the fluid. An expression is proposed for the hindrance function quantifying the dependence of the particle settling velocity on the surface particle concentration. Of interest is the evolution of the axial concentration profile when the particles are acted upon by an external force, whose magnitude is proportional to a single-particle settling velocity directed towards the stationary disk.

We find that the combined effect of the particle sedimentation and of the large extensional velocity during necking leads to particle stratification. In addition to the expected concentration peak near the stationary disk, a second concentration peak develops between the neck and the moving disk. There exist a critical settling velocity for which this peak crosses the neck before pinch-off. We propose an expression for the hindrance function modelling the dependence of the particle settling speed on the particle concentration. Analogously to bulk sedimentation, this models predicts a sharpening of the concentration gradients.

The form of the transport equations for the particle phase discussed in this paper does not rely on phenomenological assumptions. Upon suitable closure, it can be applied to study non-trivial hydrodynamic and non-hydrodynamics (e.g. electrostatic) forces between particles on generally curved interfaces. Studying these interactions with the formulation presented here represents a fruitful avenue of research. The main limitation of the current study is the one-way coupling assumption. A large body force on the particles should give appreciable deformations of the interface. It is possible to model this effect by suitably modifying the thin-thread equation for the fluid in the liquid bridge. This modification is the subject of current work.

References

[1] A. Rapacchietta, A. Neumann, Force and free-energy analyses of small particles at

fluid interfaces: II. Spheres, J. Colloid Interface Sci. 59 (3) (1977) 555 – 567.

[2] P. A. Kralchevsky, K. Nagayama, Capillary interactions between particles bound to interfaces, liquid films and biomembranes, Adv. Colloid Interface Sci. 85 (1993) 145.

[3] P. Singh, D. D. Joseph, Fluid dynamics of floating particles, J. Fluid Mech. 530 (2005) 31–80.

[4] L. Botto, E. P. Lewandowski, M. Cavallaro, K. J. Stebe, Capillary interactions between anisotropic particles, Soft Matter 8 (2012) 9957–9971.

[5] M. Abkarian, S. Protire, J. M. Aristoff, H. A. Stone, Gravity-induced encapsulation of liquids by destabilization of granular rafts, Nat. Commun. 4 (2013) 1985.

[6] E. G. Kim, K. Stratford, P. S. Clegg, M. E. Cates, Field-induced breakup of emulsion droplets stabilized by colloidal particles, Phys. Rev. E 85 (2012) 020403.

[7] J. W. Tavacoli, G. Katgert, E. G. Kim, M. E. Cates, P. S. Clegg, Size limit for particle-stabilized emulsion droplets under gravity, Phys. Rev. Lett. 108 (2012) 268306.

[8] X. Zhang, R. Padgett, O. Basaran, Nonlinear deformation and breakup of stretching liquid bridges, J. Fluid Mech. 329 (1996) 207–245.

[9] S. Gaudet, G. McKinley, H. Stone, Extensional deformation of Newtonian liquid bridges, Phys. Fluids 8 (10) (1996) 2568–2579.

[10] Y.-C. Liao, E. I. Franses, O. A. Basaran, Deformation and breakup of a stretching liquid bridge covered with an insoluble surfactant monolayer, Phys. Fluids 18 (2) (2006) 022101.

[11] B. Ambravaneswaran, O. A. Basaran, Effects of insoluble surfactants on the nonlinear deformation and breakup of stretching liquid bridges, Phys. Fluids 11 (5) (1999) 997–1015.

[12] P. R. Nott, J. F. Brady, Pressure-driven flow of suspensions: simulation and theory, J. Fluid Mech. 275 (1) (1994) 157–199.

[13] D. Drew, Mathematical modeling of two-phase flow, Ann. Rev. Fluid Mech. 15 (1) (1983) 261–291.

[14] R. Aris, Vectors, tensors and the basic equations of Fluid Mechanics, Courier Dover Publications, 2012.

[15] G. Batchelor, The stress system in a suspension of force-free particles, J. Fluid Mech. 41 (03) (1970) 545–570.

[16] C. Pozrikidis, Particle motion near and inside an interface, J. Fluid Mech. 575 (2007) 333–357.

[17] J. Eggers, T. F. Dupont, Drop formation in a one-dimensional approximation of the Navier–Stokes equation, J. Fluid Mech. 262 (1994) 205–221.

[18] R. Kröger, S. Berg, A. Delgado, H. Rath, Stretching behaviour of large polymeric and Newtonian liquid bridges in Plateau simulation, J. Non-Newtonian Fluid Mech. 45 (3) (1992) 385–400.

[19] A. M. Davis, E. Lauga, Hydrodynamic friction of fakir-like superhydrophobic surfaces, J. Fluid Mech. 661 (2010) 402–411.

[20] K. Ranger, The circular disk straddling the interface of a two-phase flow, Int. J. Multiphase Flow 4 (3) (1978) 263–277.